78–88 *Nucleic Acids Research, 2006, Vol. 34, No. 1*
doi:10.1093/nar/gkj415

Evolutionary-conserved telomere-linked helicase genes of fission yeast are repressed by silencing factors, RNAi components and the telomere-binding protein Taz1

Klavs R. Hansen, Pablo Tejero Ibarra and Geneviève Thon*

Department of Genetics, Institute of Molecular Biology and Physiology, University of Copenhagen, Denmark

Received September 19, 2005; Revised and Accepted December 12, 2005

ABSTRACT

In *Schizosaccharomyces pombe* the RNAi machinery and proteins mediating heterochromatin formation regulate the transcription of non-coding centromeric repeats. These repeats share a high sequence similarity with telomere-linked helicase (*tlh*) genes, implying an ancestral relationship between the two types of elements and suggesting that transcription of the *tlh* genes might be regulated by the same factors as centromeric repeats. Indeed, we found that mutants lacking the histone methyltransferase Clr4, the Pcu4 cullin, Clr7 or Clr8, accumulate high levels of *tlh* forward and reverse transcripts. Mutations and conditions perturbing histone acetylation had similar effects further demonstrating that the *tlh* genes are normally repressed by heterochromatin. In contrast, mutations in the RNAi factors Dcr1, Ago1 or Rdp1 led only to a modest derepression of the *tlh* genes indicating an alternate pathway recruits heterochromatin components to telomeres. The telomere-binding protein Taz1 might be part of such a redundant pathway, *tlh* transcripts being present at low levels in Δ*taz1* mutants and at higher levels in Δ*taz1* Δ*dcr1* double mutants. Surprisingly, the chromodomain protein Chp1, a component of the Ago1-containing RITS complex, contributes more to *tlh* repression than Ago1, indicating the repressive effects of Chp1 are partially independent of RITS. The *tlh* genes are found in the subtelomeric regions of several other fungi raising the intriguing possibility of conserved regulation and function.

INTRODUCTION

The heterochromatic regions associated with the centromeres of many higher eukaryotes contain an abundance of repeats originating from transposable elements. The epigenetic association of these centromeric regions with particular sets of proteins is in some respects more critical to centromere function than specific DNA sequences as indicated e.g. by the properties of neocentromeres [reviewed in (1)].

In spite of their relatively small size of ∼40–100 kb, the three *Schizosaccharomyces pombe* centromeres resemble those of higher eukaryotes [reviewed in (2)]. Their central cores (*cnt)* are associated with the CENH3/CenpA protein, a hallmark of eukaryotic centromeres defining the region of kinetochore attachment. The central cores are flanked by repeated sequences packaged into heterochromatin, the inner most (*imr*) and outer repeats (*otr*). The *otr* can in turn be subdivided into two types of repeats whose relative positions differ between the three centromeres (3–8), designated here *dh* and *dg* repeats (Figure 1A). Both inner and outer repeats are required for efficient chromosome segregation (9,10) as are components of heterochromatin [reviewed in (2)]. The origin of centromeric repeats is not known.

A *dh-dg* repeat unlinked to centromeres is found in the silenced part of the mating-type region. This particular element has been designated *cenH*, for centromeric homology (11). *cenH* facilitates heterochromatin formation in the mating-type region by recruiting the histone methyltransferase (HMT) Clr4 and the chromodomain protein Swi6 (12–15). All or parts of *cenH* can also promote heterochromatin formation at an ectopic site (16) as can fragments derived from centromeric DNA (17).

The centromeric *dh* and *dg* repeats and *cenH* have been implicated in RNAi-dependent heterochromatin formation (15,18–20). In *S.pombe* the RNAi pathway involves a member

*To whom correspondence should be addressed at Department of Genetics, Institute of Molecular Biology and Physiology, University of Copenhagen, Øster Farimagsgade 2A, 1353 Copenhagen K, Denmark. Tel: +45 35 32 21 08; Fax: +45 35 32 21 13; Email: gen@my.molbio.ku.dk

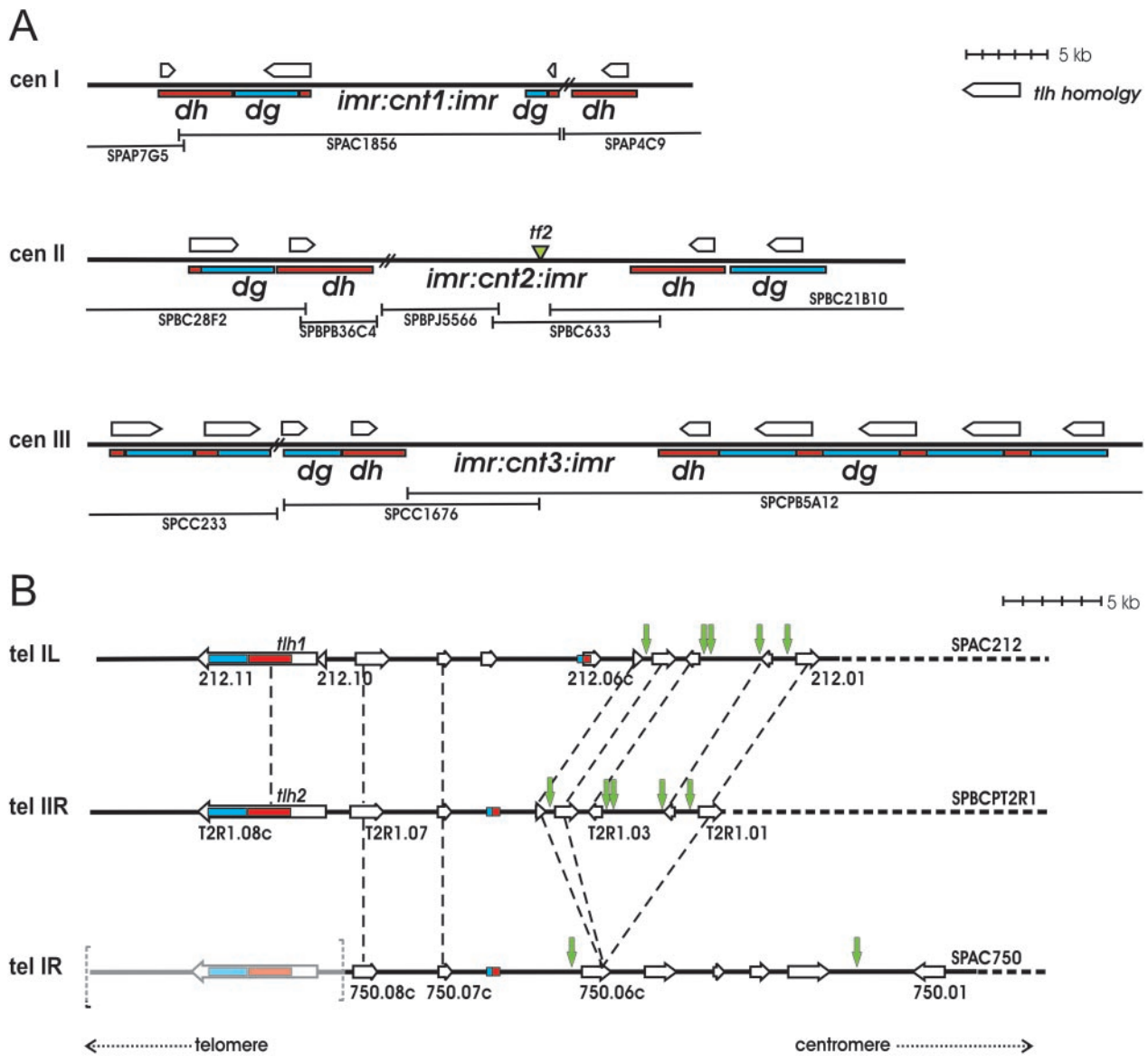

Figure 1. Regions of sequence homology in *S.pombe* centromeres and subtelomeres. (**A**) Schematic representation of *S.pombe* centromeres. *dh* and *dg* repeats are indicated in red and blue, respectively. Regions of homology (>60% sequence identity) between *tlh* genes and centromeric repeats are indicated by open arrows. These regions map within 3921 bp in the 5662 bp *tlh1* ORF, 1102 bp (seven segments; <2% gap) of *tlh1* displaying an identity to centromeric sequences >75%. Centromeric repeats that have not been sequenced are indicated by double bars. *dh* and *dg* repeats were placed according to published data (8) and our own sequence comparisons. The green arrowhead indicates a previously unidentified fragment from a *tf2*-retrotransposable element. Available cosmid sequences (8) are represented by bars below each centromere. (**B**) Schematic representation of *S.pombe* subtelomeric regions. The subtelomeric cosmids SPAC212, SPBCPT2R1 and SPAC750 are represented. Dashed lines between SPAC212, SPBCPT2R1 and SPAC750 point to regions of synteny. The *tlh* homology to centromeric repeats is represented in red (*dh*) or blue (*dg*). Green arrows indicate the presence of LTRs. Open arrows denote ORFs. Bracketed grey lines in the left portion of tel1R represent a hypothetical *tlh* gene that is not part of the SPAC750 sequence. Its presence and position are suggested by hybridization experiments (35) and by the syntenic relationship between the three represented telomeres (see text).

of the Argonaute family (Ago1), an RNase III-like enzyme (Dcr1) and an RNA-dependent RNA polymerase (Rdp1). Ago1 is part of a ribonucleoprotein complex called RITS for RNA-induced initiation of transcriptional silencing complex. In addition to Ago1, RITS contains the Tas3 protein, the chromodomain protein Chp1 and 20–22 nt RNA molecules (siRNA) mostly originating from centromeric *dh* and *dg* repeats (21–23). Rdp1 participates in a different complex, the RNA-directed RNA polymerase complex or RDRC, capable of interacting with RITS and containing the RNA helicase Hrr1 and Cid12, a member of the poly(A) polymerase family (22). Rdp1, Dcr1, Ago1, Chp1, Tas3, Hrr1 and Cid12 are major players in the formation of centromeric heterochromatin (19,21,22,24–26). According to all available evidence, double-stranded RNAs produced by either the bi-directional transcription of centromeric repeats, or by RDRC acting on centromeric transcripts, are processed into siRNA by Dcr1 and one strand is incorporated into the RITS complex. Early models proposed that the primary function of RITS and its components was to direct heterochromatin

formation to chromosomal regions with homology to the small single-stranded RNA molecules contained in the complex (15,21). It has become increasingly clear however that the association of RITS with chromatin depends on histone H3 lysine 9 methylation (H3K9Me) whereas H3K9Me can be formed in cells lacking RNAi components (27,28). The current view is therefore that H3K9Me serves as an anchor for Chp1, tethering RITS and RDRC to heterochromatin and allowing these complexes to propagate existing heterochromatin rather than, or in addition to, establishing its formation (17,22,29,30). Histones are deacetylated in the marked regions by the Clr3 and Clr6 deacetylases and histone H3 is methylated at K9 by the Clr4 methyltransferase, the molecular mechanisms linking these events to RITS or RDRC remaining unknown.

The RITS component Chp1 associates not only with centromeric heterochromatin but also with the mating-type region and telomeres (23,28,29). In contrast to its role at centromeres, however, Chp1 is not essential to heterochromatin formation or transcriptional silencing in the mating-type or telomeric regions (25,28,29). In the mating-type region, Chp1 facilitates silencing in a manner redundant with the DNA-binding protein Atf1 (31,32). Similarly, Chp1 might promote silencing in telomeric and subtelomeric regions in a manner redundant with some other factor, possibly the telomeric-repeat binding protein Taz1 (33).

We report here our characterization of subtelomeric sequences sharing a high similarity with the *dh-dg* centromeric repeats and *cenH* element. These sequences are part of the open reading frames (ORFs) of putative telomere-linked helicases (Tlh) of the RecQ family. Expression of the *tlh* genes is induced in cells undergoing telomere crisis caused by the loss of telomerase (34). Furthermore, the ectopic expression of part of a *tlh* ORF speeds up recovery from crisis (35) indicating a role in telomere rescue under this extreme condition. The level of *tlh* RNA is naturally low in wild-type cells that are not undergoing crisis and this low level has been proposed to be brought about by RNAi (34). We examined the transcriptional regulation of the *tlh* genes in greater detail, determining the relative contributions of histone-modifying enzymes, RNAi components, and of the telomere-binding protein Taz1 to their expression level. Furthermore, we determined that related ORFs are present in the subtelomeric regions of other fungi, suggesting an evolutionary-conserved function and mode of regulation for the *tlh* genes.

MATERIALS AND METHODS

S.pombe strains and media

The strains used in this study and their genotypes are listed in Table 1. Media were as described previously (13).

Cultures for RNA extractions

Unless indicated otherwise, cells were propagated in 25–50 ml YES medium at 30°C and collected while in their exponential growth phase by a 3 min centrifugation at 3000 r.p.m. in a Heraeus megafuge 2R. The cell pellets were frozen in liquid nitrogen immediately after centrifugation and stored at −80°C until further processing. For the nitrogen starvation experiments, 200 ml cultures growing exponentially in YES ($\sim 5 \times 10^6$ cells/ml) were spun down by a 3 min centrifugation at 3000 r.p.m. The cells were washed once in 25 ml MSL-N pre-warmed to 30°C, resuspended at $\sim 5 \times 10^6$ cells/ml in MSL-N supplemented with 100 mg/l adenine, 100 mg/l uridine and 200 mg/l leucine, and placed back on a shaking platform at 30°C. At each time point $\sim 1 \times 10^8$ cells were collected by centrifugation for RNA extraction.

Table 1. Strains and their genotypes

J11	*h*$^{+N}$ *leu1-32 ura4-D18 ade6-M216 taz1::ura4*$^+$
PG2870	*h*$^{+N}$ *leu1-32 ura4-D18 ade6-M210 chp1::LEU2*
PG3039	*h*$^{-S}$ *ura4-D18 dcr1::kan*^{R}
PG3267	*h*$^{-S}$ *leu1-32 ade6-DN/N [ura4*$^+$*-tlh2-ade6*$^+$*]*
PG3269	*h*$^{-S}$ *leu1-32 ade6-DN/N [ura4*$^+$*-2hlt-ade6*$^+$*]*
PG3273	*h*$^{-S}$ *leu1-32 ade6-DN/N [ura4*$^+$*- tlh1-ade6*$^+$*]*
PG3275	*h*$^{-S}$ *leu1-32 ade6-DN/N [ura4*$^+$*-1hlt-ade6*$^+$*]*
PG3389	*h*$^{+N}$ *otr1R(SphI)::ura4*$^+$ *leu1-32 ura4-DS/E ade6-M210 clr8Δ::kan*^{R}
PG3435	*h*^{90} *ura4-D18 pcu4::ura4*$^+$
PTI3	*h*^{90} *leu1-32 ura4-DS/E ade6-DN/N*
PTI14	*h*$^{-S}$ *leu1-32 ade6-DN/N [ura4*$^+$*-ade6*$^+$*]*
SPA15	*h*$^{-S}$ *otr1R(SphI)::ura4*$^+$ *leu1-32 ura4-DS/E ade6-M210 clr7Δ::kan*^{R}
SPK10	*h*$^{-S}$
SPK20	*h*$^{-S}$ *ura4-D18 clr4::ura4*
SPK27	*h*$^{-S}$ *clr6-1 clr3::kan*^{R}
SPK50	*h*$^{+N}$ *ura4-D18 leu1-32 dcr1::kan*^{R}
SPK51	*h*$^{-N}$ *ura4-D18 ade6-M216 taz1:: ura4*$^+$
SPK52	*h*$^{+N}$ *ura4-D18 leu1-32 dcr1::kan*^{R}
SPK53	*h*$^{-N}$ *ura4-D18 ade6-M216 taz1:: ura4*$^+$
SPK54	*h*$^{-S}$ *ura4-D18 ade6-M216*
SPK55	*h*$^{+N}$ *ura4-D18 leu1-32 dcr1::kan*^{R} *taz1:: ura4*$^+$
SPK56	*h*$^{+N}$ *ura4-D18 ade6-M216 leu1-32*
SPK57	*h*$^{-S}$ *ura4-D18::kan*^{R} *taz1:: ura4*$^+$
SPK61	*h*$^{-S}$ *ura4-D18 ade6-M216 dcr1::kan*^{R} *taz1:: ura4*$^+$
TV292	*h*$^{-S}$ *ura4-DS/E ago1::kan*^{R}
TV293	*h*$^{-S}$ *ura4-DS/E dcr1::kan*^{R}
TV296	*h*$^{-S}$ *ura4-DS/E rdp1::kan*^{R}

Treatments with Trichostatin A (TSA)

TSA treatments were performed by adding 35 μg/ml TSA (US Biologicals) to exponentially growing 5 ml YES cultures that had reached $\sim 5 \times 10^6$ cells/ml and incubating the cultures for 24 h on a shaking platform at 30°C. The cells were then spun down by a 3 min centrifugation at 3000 r.p.m., washed once in 10 ml YES pre-warmed to 30°C, and used to inoculate 25 ml YES recovery cultures. Cells in recovery cultures were examined daily under a microscope, counted and used to inoculate fresh cultures. The cultures were diluted ~250-fold each day. Cells ($\sim 1 \times 10^8$) were collected for RNA extractions at the indicated time points. In the case of PG3267 and PG3273 suspensions of cells in their repressed state were divided in two. One half was treated with TSA for 24 h as described above while the other half was mock treated. Following treatment, cells were plated on AA medium lacking adenine or containing 15 mg/l adenine. The plates were incubated at 33°C for 4 days and photographed. The experiment was conducted in triplicate using three independent cultures of each PG3267 and PG3273.

Plasmid and strain constructions

pPTI1, a plasmid containing a full-length *ade6*$^+$ gene flanked by DNA originating from the *ura4*$^+$ locus, was created by ligating

into Bluescript SKII(−) (Stratagene) (i) a 645 bp SacI–EagI fragment created by PCR with GTO-212 (GGGAGCTCGAGGGTATTATACAAGGC), GTO-213 (GGACGGCCGTGTGGTAATGTTGTAGGAG) and a 1.8 kb HindIII template containing *ura4*$^+$ and flanking sequences (36); (ii) the 2735 bp EaeI–SpeI fragment of pAS1 (37) containing the *ade6*$^+$ gene, and (iii) a 201 bp SpeI–KpnI fragment created by PCR with GTO-214 (GGACTAGTATCTTTTCTCTGGATTGAC), GTO-215 (GGGGTACCTGACGAAACTTTTTGACATC) and the 1.8 kb *ura4*$^+$ template. The predicted ORFs of *tlh1* and *tlh2* were amplified from genomic DNA of *S.pombe* 968 cells (h^{90}) using OKR63 (TTAGGCCTCGGCCGATGGTCGTCGCTTCAGAAATTGC) and OKR64 (TTAGGCCTCGGCCGCGATATGAAACGTTGTCTTGCATCAG) or OKR65 (TTAGGCCTCGGCCGGCGTGTACTATGGCAACTGGTGGTGTTGGCTTG) and OKR64 and the Expand PCR system (Roche). The PCR products were cloned into the pCRII-TOPO vector (Invitrogen), excised by EagI digestion, and inserted in either orientation into the EagI site of pPTI1 to create pKR44 (OKR63-OKR64 fragment with OKR64 close to ura4$^+$); pKR45 (OKR63-OKR64 fragment with OKR63 close to ura4$^+$); pKR48 (OKR64-OKR65 fragment with OKR64 close to ura4$^+$); and pKR49 (OKR64-OKR65 fragment with OKR65 close to ura4$^+$). The four plasmids and pPTI1 were digested with SacI and KpnI to release their inserts and used to transform the *S.pombe* strain PTI1. Ade$^+$ transformants were selected on AA-ade plates. To take into account the possibility that the *tlh* genes might repress transcription of *ade6*$^+$, both fast and slow growing Ade$^+$ transformants were examined by Southern blot. Several transformants containing correct chromosomal integrations at the *ura4*$^+$ locus were identified in this way for each construct including PG3267 with pKR49 (*ura4*$^+$-*tlh2-ade6*$^+$), PG3269 with pKR48 (*ura4*$^+$-*2hlt-ade6*$^+$), PG3273 with pKR45 (*ura4*$^+$-*tlh1-ade6*$^+$), PG3275 with pK44 (*ura4*$^+$-*2hlt-ade6*$^+$), and PTI14 with pPTI1 (*ura4*$^+$-*ade6*$^+$).

Microscopy

DIC images were obtained using a Zeiss Axio Imager fluorescence microscope equipped with a Hamamatsu Orca-ER digital camera and Volocity 3.5.1 software.

RNA extraction, RT–PCR and real-time PCR

RNA was extracted with a hot-phenol procedure as described previously (38). Detection of centromeric transcripts by RT–PCR was performed as in Ref. (19) using GTO-223 (GAAAACACATCGTTGTCTTCAGAG) and GTO-226 (TCGTCTTGTAGCTGCATGTGA). *tlh dh* transcripts were amplified with OKR40 (TCGTCTTGTAGCAGCATGTGA) and OKR41 (GAGATGAACGTATCTCTATCGAC); *tlh DEAH* transcripts with OKR44 (CTGGAGGTGGAAAGTCTTTGTCG) and OKR45 (AACCGAAGACCACTGTTGGTTAATGC); actin transcripts with OKR70 (GGCATCACACTTTCTACAACG) and OKR71 (GAGTCCAAGACGATACCAGTG). OKR70 and OKR71 were also used for −RT controls. Strand specificity was achieved by using a single primer in the reverse transcription: GTO-226 for the centromeric forward transcript, GTO-223 for the centromeric reverse transcript; OKR41 for the *tlh dh* forward transcript; OKR40 for the *tlh dh* reverse transcript; OKR45 for the *tlh DEAH* forward transcript; and OKR44 for the *tlh DEAH* reverse transcript. For the amplification of centromeric or telomeric transcripts 27 PCR cycles were performed, and 25 cycles for the amplification of actin transcripts.

Real-time PCR was performed with a BioRad iCycler using the Quantitect SYBR Green RT–PCR mixture (Qiagen) supplemented with 10 nM Fluorescein (BioRad). Reverse transcriptions of ∼90 ng total RNA were allowed to take place at 50°C for 30 min in 25 µl reactions. The reverse transcription step was followed by 15 min at 95°C to inactivate the RT and activate the HotStarTaq polymerase. cDNAs were then amplified by 40 cycles of (30s 94°C; 45s 56°C; 60s 72°C). The OKR40 and OKR41 primers were used for *tlh* amplification, and OKR70 and OKR71 for actin amplification. All primers were used at a final concentration of 0.6 µM. The melting curve of each sample was determined after amplification. Reactions were set up in triplicate. Three-fold dilution series of genomic DNA were used to determine the efficiency of amplification for each primer pair by plotting standard curves. Mean normalized expression (MNE) values were calculated according to Equation 1 and standard errors on the mean (SE_{MNE}) according to Equation 2 (39).

$$\mathrm{MNE} = \frac{(E_{\mathrm{reference}})^{\mathrm{CT}_{\mathrm{reference,mean}}}}{(E_{\mathrm{target}})^{\mathrm{CT}_{\mathrm{target,mean}}}}, \quad \mathbf{1}$$

$$\mathrm{SE}_{\mathrm{MNE}} = \mathrm{MNE}\cdot[(\ln(E_{\mathrm{target}})\cdot\mathrm{SE}_{\mathrm{CT}_{\mathrm{target,mean}}})^2 + (\ln(E_{\mathrm{reference}})\cdot\mathrm{SE}_{\mathrm{CT}_{\mathrm{reference,mean}}})^2]^{1/2}, \quad \mathbf{2}$$

where $E_{\mathrm{reference}}$ is the efficiency of actin amplification, E_{target} the efficiency of *tlh* amplification, $\mathrm{CT}_{\mathrm{reference,\ mean}}$ the mean cycle threshold value for actin, and $\mathrm{CT}_{\mathrm{target,\ mean}}$ the mean cycle threshold value for *tlh*.

DNA and protein sequence analyses

Sequence analyses were performed using online available BLAST (40) services from the Sanger Institute (www.sanger.ac.uk), Broad Institute (www.broad.mit.edu), Genolevures (cbi.labri.u-bordeaux.fr/Genolevures) and NCBI (www.ncbi.nlm.nih.gov). Multiple alignments were created using ClustalW (41) at EBI (www.ebi.ac.uk). The cladogram presented in Figure 2 was manually edited using NJPLOT (42).

RESULTS AND DISCUSSION

The centromeric *dh* and *dg* repeats share sequence homology with subtelomeric helicase genes

The *dh* and *dg* repeats found at centromeres and in the mating-type region display extensive sequence homology with large telomeric ORFs encoding putative helicases of the recQ family (Figure 1) (8,34). The *t*elomere-*l*inked *h*elicase (*tlh*) ORFs are the last ORFs in the subtelomeric regions of chromosome I (SPAC212.11 or *tlh1*) and chromosome II (SPBCPT2R1.08c or *tlh2*). In addition to the high sequence similarity shared by *tlh1* and *tlh2* a significant conservation is observed between the ORFs neighboring *tlh1* and *tlh2* indicating the two subtelomeric regions resulted from a duplication (Figure 1B). A region partly similar to the duplicated sequence is also found in the right subtelomere of chromosome I suggesting that ORFs homologous to *tlh1*/*tlh2* might exist there as well in

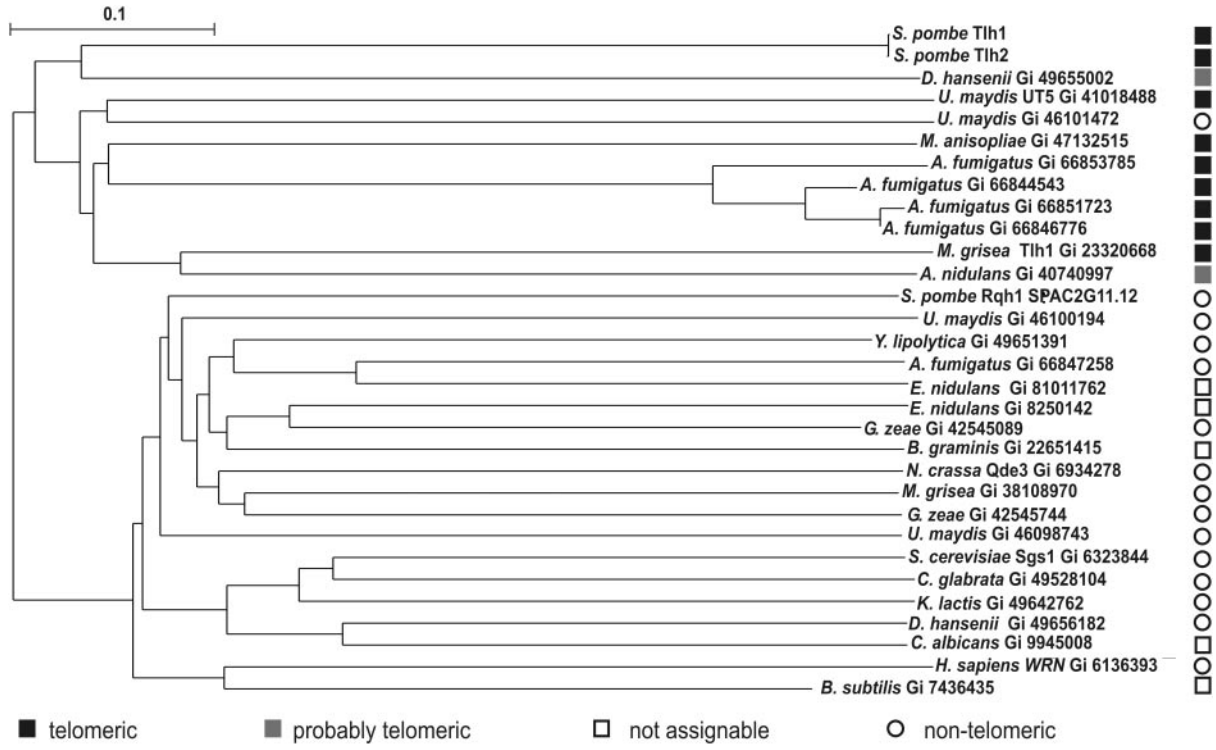

Figure 2. Conservation of *tlh* genes in fungi. The displayed subtree was created from a full alignment including the product of 58 *S.pombe* helicase genes and 42 RecQ helicases from other species (see text). Black squares mark the products of telomeric ORFs (according to annotations); grey squares mark ORFs that are first or second in contigs >500 kb; open circles mark ORFs that are more than two ORFs away from the end of a DNA segment; and open squares mark single ORFs not assigned to any segment, or bacterial ORFs.

a region whose sequence has not been completed yet. This hypothesis is supported by hybridization experiments (34). Similar ORFs are not present in the sequenced chromosome III, the telomeric repeats in chromosome III being immediately adjacent to rDNA repeats (8).

The sequence similarity between *tlh1* and *tlh2* is greater than 99% in a 5757 nt long region. The high sequence conservation between *tlh1* and *tlh2* might be maintained by frequent gene conversions between subtelomeric regions that are known to cluster early in meiosis promoting the alignment of homologous chromosomes [reviewed in (43)]. Consistent with frequent physical exchanges during meiosis, we observed 3:1 segregations of restriction fragment length polymorphisms at the *tlh* genes in tetrad dissections (data not shown).

In addition to SPAC212.11 and SPBCPT2R1.08c, truncated *tlh* copies are present near the full-length genes in the two subtelomeric regions. These truncated ORFs are unlikely to encode functional proteins. However, they might serve as structural components similar to the *otr* repeats at centromeres.

Conservation of *tlh* genes in fungi

We used ClustalW to compare Tlh1 with a set of related proteins. This set comprised 40 protein sequences identified in a BLAST search performed with Tlh1 against the Fungi database at NCBI (Matrix: BLOSUM62; Gap Costs: Existence: 11, Extension:1; *E*-value $\leqslant 1 \times 10^{-13}$), the protein products of all *S.pombe* helicase genes (58 sequences), RecQ from *Bacillus subtilis*, and the human RecQ homologue WRN. All RecQ helicases clustered in a subtree apart from the non-recQ helicases of *S.pombe* (data not shown). The RecQ subtree could be divided into two main branches (Figure 2), one containing among others human WRN and *S.pombe* Rqh1, and the other primarily containing proteins encoded by telomere-linked genes: *S.pombe* Tlh1 and Tlh2; *Ustilago maydis* UT5 (44); *Metarhizium anasopliae* TAH1 (45); *Magnaporthe grisea* Tlh1 (46); and four telomeric helicases from *Aspergillus fumigatus* (Gi 66853785, 66844543, 66851723 and 66846776). In addition, the latter branch contained two proteins from *Aspergillus nidulans* (Gi 40740997) and *Debaryomyces hansenii* (Gi 49655002), respectively, both encoded by the second last ORF in segments >500 kb. According to their position in the contigs and sequence similarity with *tlh1* and *tlh2* these two genes might be novel *tlh* genes encoding homologues of *S.pombe tlh1* and *tlh2* in *A.nidulans* and *D.hansenii*.

The subtelomeric Y′ elements of *Saccharomyces cerevisiae* also encode helicases (47,48). The Y′ ORFs are very distantly related to the *S.pombe tlh* genes; however, they might fulfill a similar function since their expression is increased in a class of telomere-crisis survivors (48), as are the *S.pombe tlh* genes (34). In both cases the helicases encoded by the subtelomeric genes possibly contribute to the resolution of defective telomere structures. Y′ elements help counteract telomere erosion in other ways by being substrates for amplification (49). Their amplification occurs by unequal recombination events (50) or following mobilization by Ty1 retrotransposons (51) and it compensates for telomere loss. The plasticity of the *tlh* genes suggests that similar mechanisms might operate in *S.pombe*.

The *tlh* genes are strictly repressed during various growth conditions

We investigated whether the *tlh* genes were expressed under stresses other than the stress caused by the loss of telomeric DNA. A large proportion of subtelomeric genes are upregulated during nitrogen starvation and repressed by heterochromatin in the presence of a good nitrogen source (52,53) suggesting that the *tlh* genes might be under a similar control. We observed however that expression of the *tlh* genes did not increase upon nitrogen starvation (Supplementary Figure 1). We also measured *tlh* expression in wild-type cells entering stationary phase in either minimal medium (EMM2) or rich medium (YES). No increase in *tlh* gene expression occurred under these conditions either (Supplementary Figure 1). This tight repression distinguishes the *tlh* genes from other subtelomeric ORFs.

The *tlh* genes are repressed by heterochromatin

tlh1 and *tlh2* displaying a strong sequence homology to well-characterized silenced regions, we investigated whether their expression was controlled by known silencing factors. *tlh* transcripts were easily detected in mutants lacking the histone acetyltransferases (HDACs) Clr3 and Clr6 or the HMT Clr4, establishing that the *tlh* genes are repressed by heterochromatin in wild-type cells (Figure 3).

A protein complex containing the Pcu4 cullin, Clr7 and Clr8 was shown recently to mediate an early step in heterochromatin formation (54–57). This complex possesses ubiquitin-ligase activity (54) and it is required for H3K9Me at centromeres and in the mating-type region (54–57). We found that the transcriptional repression of the *tlh* genes was strongly dependent on Pcu4, Clr7 and Clr8 (Figure 3B). Deletion of any of these factors resulted in an increase in *tlh* forward and reverse transcript comparable with the increase in cells lacking Clr4. This derepression is consistent with Pcu4, Clr7 and Clr8 controlling histone methylation and transcription of the *tlh* genes similar to the control they exert in the mating-type and centromeric regions.

Transcripts originating from both strands could be detected in Δ*clr4*, *clr6-1*Δ*clr3*, Δ*pcu4*, Δ*clr7* and Δ*clr8* mutants (Figure 3), reminiscent of the situation at centromeres (19). When using primers amplifying the region with highest *dh* homology (OKR40 and OKR41), we detected similar levels of forward and reverse strand transcripts in derepressed mutants (Figure 3C). However, when using primers further toward the

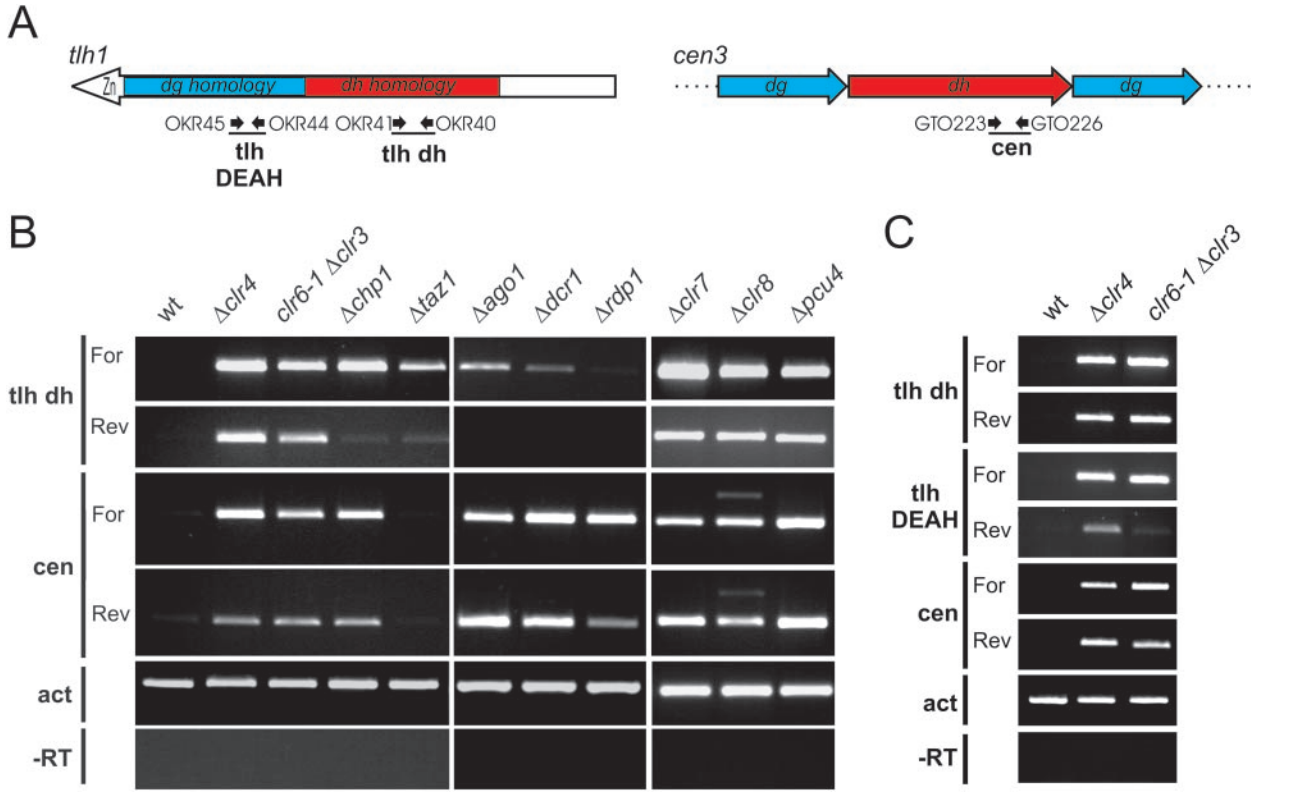

Figure 3. Transcriptional regulation of the *S.pombe tlh* genes. (**A**) Schematic representation of the *tlh1* gene and of a portion of centromere 3 indicating the location of primers used in (B and C) and fragments amplified with these primers. (**B**) Abundance of forward and reverse *tlh* transcripts in heterochromatin, RNAi and Taz1 mutants. Strand specific RT–PCR was performed to estimate the levels of *tlh* RNA by amplifying a region of *tlh* with high sequence similarity to the centromeric *dh* repeats (tlh dh). Reverse transcription was primed with OKR41 to detect the *tlh* forward strand (For), or with OKR40 to detect the *tlh* reverse strand (Rev). Centromeric forward (cen For) and reverse (cen Rev) RNAs were detected as described previously (19). The bands observed above the centromeric forward and reverse PCR products in the Δ*clr8* panels originate from the mating-type region in h^{90} strains. The actin transcript (act) was amplified to estimate the amount of total RNA in the samples. −RT was performed with actin primers. wt:SPK10; Δ*clr4*:SPK20; *clr6-1*Δ*clr3*:SPK27; Δ*chp1*:PG2870; Δ*taz1*:J11; Δ*ago1*:TV292; Δ*dcr1*:TV293; Δ*rdp1*:TV296; Δ*clr7*:SPA15; Δ*clr8*:PG3389; Δ*pcu4*:PG3435. (**C**) Variations in the abundance of reverse strand along the *tlh* ORF. RT–PCR was performed as in (A). In addition, a region of *tlh* RNA encoding the DEAH helicase domain (tlh DEAH) was amplified, the reverse transcription being primed with OKR45 to detect the forward strand (For) or with OKR44 to detect the reverse strand (Rev).

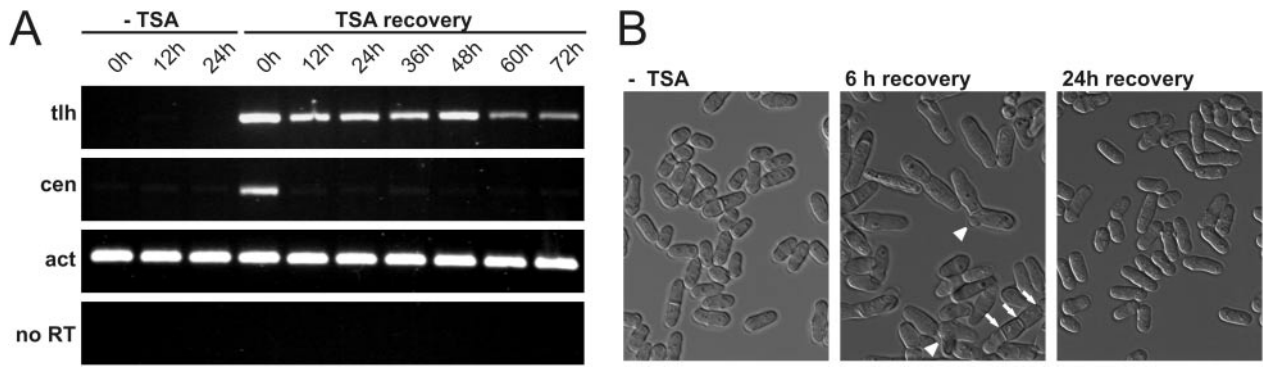

Figure 4. Recovery from TSA treatment. (**A**) Centromeric and subtelomeric RNAs in cells recovering from TSA treatment. RT–PCR was performed on wild-type cells (SPK10) not treated with TSA (−TSA), or treated with TSA and maintained in culture for the indicated times following TSA removal (+TSA). (**B**) Normal cell morphology (−TSA) is perturbed by TSA treatment (6 h recovery) and re-established within a few generations following TSA removal (24 h recovery). White arrowheads point to cases of pseudohyphal growth and white arrows to multiple septa in a single cell.

3′ end of the *tlh* genes where the sequence similarity to centromeric repeats is less pronounced (OKR44 and OKR45) we observed significantly lower levels of the reverse strand transcript than of the forward transcript, suggesting that reverse strand synthesis is initiated within the *tlh* ORF and primarily occurs near the strongest *dh* homology.

Derepresssion of the *tlh genes by* TSA

Treatment with the histone deacetylase inhibitor TSA caused an accumulation of *tlh* transcripts similar to the level observed in the *clr6-1*Δ*clr3* HDAC double mutant (Figure 4). This derepression further supports the notion that histone deacetylation is a critical determinant of *tlh* gene regulation. TSA treatment had a similar effect upon centromeric silencing, leading to an accumulation of non-coding transcripts from centromeric repeats (Figure 4).

Following TSA removal, the kinetics of repression differed markedly at centromeres and telomeres. Centromeric silencing was re-established within 12 h, whereas the *tlh* genes were still expressed as long as 72 h after TSA removal. Dramatic changes in cell morphology accompanied TSA treatment. Six hours after TSA removal nearly all cells were elongated with multiple septa and a substantial fraction were undergoing pseudo-hyphal growth. These morphological changes likely reflect global changes in gene expression resulting from the loss of HDAC activity (53). Cell morphology had returned to normal 24 h after TSA removal indicating the global effects of TSA treatment had faded at that time, consistent with the restored centromeric silencing. Hence, the long-term derepression of the *tlh* genes by TSA treatment appears very specific for these genes. This effect points to histone deacetylation as a key epigenetic mark controlling the expression of the *tlh* genes, and to an inefficient mechanism of heterochromatin establishment in subtelomeric regions.

Heterochromatin formation at the *tlh* loci

The levels of *tlh* transcripts were reported recently to be controlled by RNAi (34). We found that in contrast to the deletion of histone-modifying enzymes, deletion of the RNAi components Ago1 or Dcr1 caused a relatively minor accumulation of the forward *tlh* transcript, the reverse strand transcript remaining undetectable (Figure 3B). Strains lacking Rdp1 did not display a noticeable increase in *tlh* forward or reverse transcripts. This is in sharp contrast with the effects of *rdp1* deletion at centromeres where non-coding transcripts accumulate (Figure 3B) (19).

Ago1 associates with the chromodomain protein Chp1 in the RITS complex (21). We assayed therefore the effect of Chp1 on *tlh* RNA levels in our attempts to assess the role of RNAi in the control of *tlh* expression. Previous reports showed that Chp1 is present at the *tlh* loci in wild-type cells, together with the H3K9Me mark and Swi6 (23,28). H3K9Me and Swi6 remain associated with *tlh,* and telomeric reporter genes remain silent in Δ*chp1* cells, supporting models where a repressive chromatin structure is formed in the absence of Chp1 (23,25,28). Surprisingly considering these previous observations, we found that forward *tlh* transcripts were relatively abundant in Δ*chp1* cells (Figure 3A). The abundance of *tlh* transcripts in Δ*chp1* cells in spite of the presence of Swi6 at the *tlh* genes indicates that forward transcription of the *tlh* genes is partially refractory to transcriptional silencing by Swi6. Surprisingly as well, the derepression caused by deleting Chp1 was more pronounced that the derepression caused by deleting Ago1 suggesting that Chp1 does not act solely in the context of RITS. One common effect of deleting Chp1 or RNAi components was that reverse transcripts were not detected in these backgrounds.

Since RNAi did not appear to be the sole, or even predominant, mechanism recruiting heterochromatin to subtelomeric regions we tested other candidates. The DNA-binding protein Taz1 associates with telomeric repeats and represses reporter genes artificially introduced in regions immediately adjacent to telomeric repeats (33,58). Thus, it appeared likely that Taz1 might affect *tlh* expression as well, possibly by recruiting silencing factors to the region. Indeed, we observed an upregulation of *tlh* transcripts in Δ*taz1* cells, primarily of the forward transcript (Figure 3B). The transcriptional repression mediated by Taz1 is therefore not restricted to the immediate vicinity of telomeres but also affects genes located ∼10 kb away from the telomeric repeats. This observation supports a model where a repressive chromatin structure nucleated by Taz1 bound to telomeric repeats spreads from the telomeres into adjacent subtelomeric regions. The derepression of the *tlh* genes in Δ*taz1* cells was not as strong as the derepression in *clr6-1*Δ*clr3* or Δ*clr4* cells (Figure 3B) indicating a

Taz1-independent pathway mediates *tlh* repression in addition to Taz1. Indeed, we found that deleting both *taz1* and *dcr1* had a cumulative derepressive effect on the *tlh* genes (Figure 5A). We further examined the expression of the *tlh* genes in the progeny of a cross between a Δ*taz1* and a Δ*dcr1* strain (Figure 5B). A slight derepression of the *tlh* genes was observed in some of the wild-type progeny (i.e. spore 2C in Figure 5B). This slight derepression reveals that silencing is slowly re-established after having been compromised by a *trans*-acting mutation, consistent with the slow re-establishment observed in cells recovering from TSA treatment (Figure 4). The *tlh* transcript levels were consistently higher in Δ*taz1*Δ*dcr1* double mutants than in single mutants reinforcing the conclusion that RNAi and Taz1 participate in redundant silencing pathways in telomeric regions. Noticeably though, the derepression observed in Δ*taz1*Δ*dcr1* double mutants was yet not as pronounced as the derepression in a Δ*clr4* mutant (Figure 5A). Other factors, such as Arp6 (59), or the products of uncharacterized genes (58) might contribute to *tlh* repression. This multiple redundancy is similar to the redundancy of silencing mechanisms in the mating-type region, where the transcription factor Atf1 and a third pathway work in parallel with RNAi to insure a full transcriptional repression of the region (31,32,60).

The *tlh* genes repress *ade6* at an ectopic site

We investigated whether the *tlh* ORFs were sufficient to establish silencing and influence the expression of neighbor genes by cloning *tlh1* and *tlh2*, respectively, upstream of an *ade6*$^+$ marker gene introduced near the native *ura4*$^+$ gene (Figure 6A and B). Both *tlh* genes repressed *ade6*$^+$, however only when the *tlh* ORF was placed in the same orientation as *ade6*$^+$. No detectable repression was observed when the *ade6*$^+$ and *tlh* ORFs diverged from each other (Figure 6A). The *ura4*$^+$ gene was still expressed following nearby insertion of the *tlh* genes. Clones with a repressed *ura4*$^+$ gene could be obtained by FOA selection (Figure 6C); however, the frequency of FOA-resistant colonies was low suggesting spreading of transcriptional silencing to *ura4*$^+$ is inefficient or alternatively raising the possibility that these clones contain additional

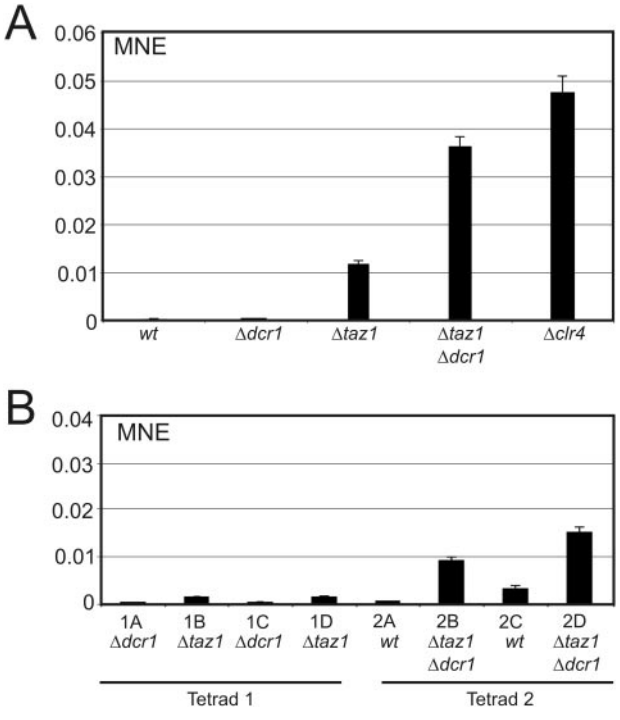

Figure 5. *tlh* RNA levels in Δ*taz1*, Δ*dcr* single and double mutants. MNE values were obtained for *tlh* transcripts by real-time RT–PCR analysis, using actin transcripts for the normalization as described in Materials and Methods. (**A**) wt:SPK10; Δ*clr4*:SPK20; Δ*taz1*Δ*dcr1*:SPK61; Δ*taz1*:J11; Δ*dcr1*:TV293. (**B**) Tetrad analysis of a cross between J11 and PG3039: Tetrad 1 (parental ditype) [Δ*dcr1*:SPK50; Δ*taz1*:SPK51; Δ*dcr1*:SPK52; Δ*taz1*:SPK53], Tetrad 2 (non-parental ditype) [wt:SPK54; Δ*taz1*Δ*dcr1*:SPK55; wt:SPK56; Δ*taz1*Δ*dcr1*:SPK57].

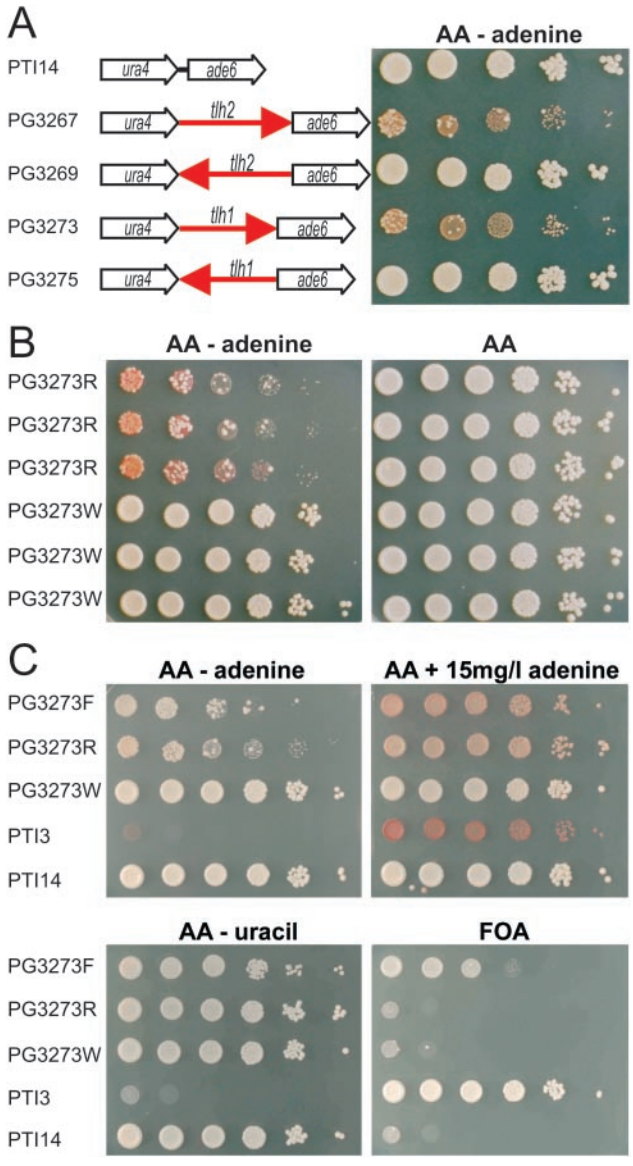

Figure 6. The *tlh* genes affect the expression of neighboring genes. (**A**) Schematic representation of constructs integrated at the *ura4* locus and phenotypes of corresponding strains. Ten-fold serial dilutions of cell suspensions were spotted on the indicated media, allowed to grow for 4 days at 33°C, and photographed. (**B**) Three individual PG3273 colonies in the red (PG3273R) or white (PG3273W) epigenetic state were spotted on the indicated media. (**C**) A FOA-resistant isolate of PG3273 (PG3273F) was plated along with a red and white isolate of the same strain and two tester strains, PTI3 (Ade$^-$ Ura$^-$) and PTI14 (Ade$^+$ Ura$^+$).

mutations affecting silencing. The epigenetic states imparted on the *ade6*$^+$ gene by *tlh1* or *tlh2* were relatively stable. The two epigenetic states conferred easily distinguishable phenotypes on media containing a low concentration of adenine, or lacking adenine (Figure 6B). Cells expressing *ade6*$^+$ form white colonies on plates containing limiting adenine concentrations while cells in which *ade6*$^+$ is repressed form red colonies. This allowed to estimate the rates of interconversion between the two states by counting half-sectored colonies. We estimated the rate of change from repressed to derepressed state at ~0.05 event per cell division (13/273 for PG3267 and 11/217 for PG3273) and the rate of change from derepressed to repressed state at ~0.001 event per cell division (1/829 for PG3267 and 1/852 for PG3273).

The existence of two interconverting epigenetic states indicated to us that the repression of *ade6*$^+$ by the *tlh* genes was mediated by heterochromatin rather than due to transcriptional interference/promoter occlusion. To confirm that this was the case, we treated cells containing an ectopic *ade6*$^+$ gene with TSA. Both PG3267 and PG3273 cells were treated and plated on medium lacking adenine and medium with a low adenine concentration (Figure 7 and data not shown). TSA treatment derepressed *tlh-ade6*$^+$ in both strains, allowing cells to form full-sized colonies on plates lacking adenine and largely white colonies on limiting adenine. This derepression is consistent with *tlh-ade6*$^+$ being regulated by histone deacetylation like the telomeric *tlh* genes.

Common ancestry of *S.pombe tlh* genes and centromeric repeats

The *dh* and *dg* repeats in centromeric and mating-type region and the telomeric *tlh* genes clearly originate from a common ancestor. Several models can be contemplated regarding the duplicative events that created these repeats. A possibility suggested by the presence of transposable elements in the pericentromeric heterochromatin of higher eukaryotes is that the *tlh* genes might be parts of transposons that preferentially transpose to heterochromatic regions. One class of putative helicase-encoding transposons called helitrons has been proposed to replicate by a rolling-circle mechanism (61). Rolling-circle replication could create tandem repeats similar those observed at *S.pombe* centromeres. Alternatively, *tlh* genes might have been mobilized with the help of retrotransposons similar to the propagation of Y′ elements in *S.cerevisiae* cells undergoing telomerase crisis (51), and the *tlh* cDNAs might have subsequently recombined with centromeric regions. A second type of event capable of creating arrangements similar to those found at centromeres would be the integration at internal chromosomal loci of elements similar to the *sod2* amplicons (62,63). The *sod2* amplicons are produced from telomeric regions and display a symmetry similar to the symmetry of centromeric regions. Yet another possibility suggested by the arrangement of the repetitive elements at centromeres and telomeres would be that *S.pombe* centromeres arose from telomere fusions (Figure 8). Numerous examples of telomere fusions have taken place in evolution, e.g. during hominoid evolution the generation of human chromosome 2 involved a telomere to telomere fusion [reviewed in (64)]. Telomeric repeats have been observed within or adjacent to pericentric regions in several avian species (65) or *Arabidopsis thaliana* (66). Similar observations were made in the genus of *Taterillus* (67). *S.pombe* cells can survive in the absence of telomerase activity by forming circularized chromosomes (68). In all characterized classes of such survivors the fused ends contain the *tlh* genes and are able to maintain heterochromatic properties in the absence of Taz1-binding sequences (69), demonstrating

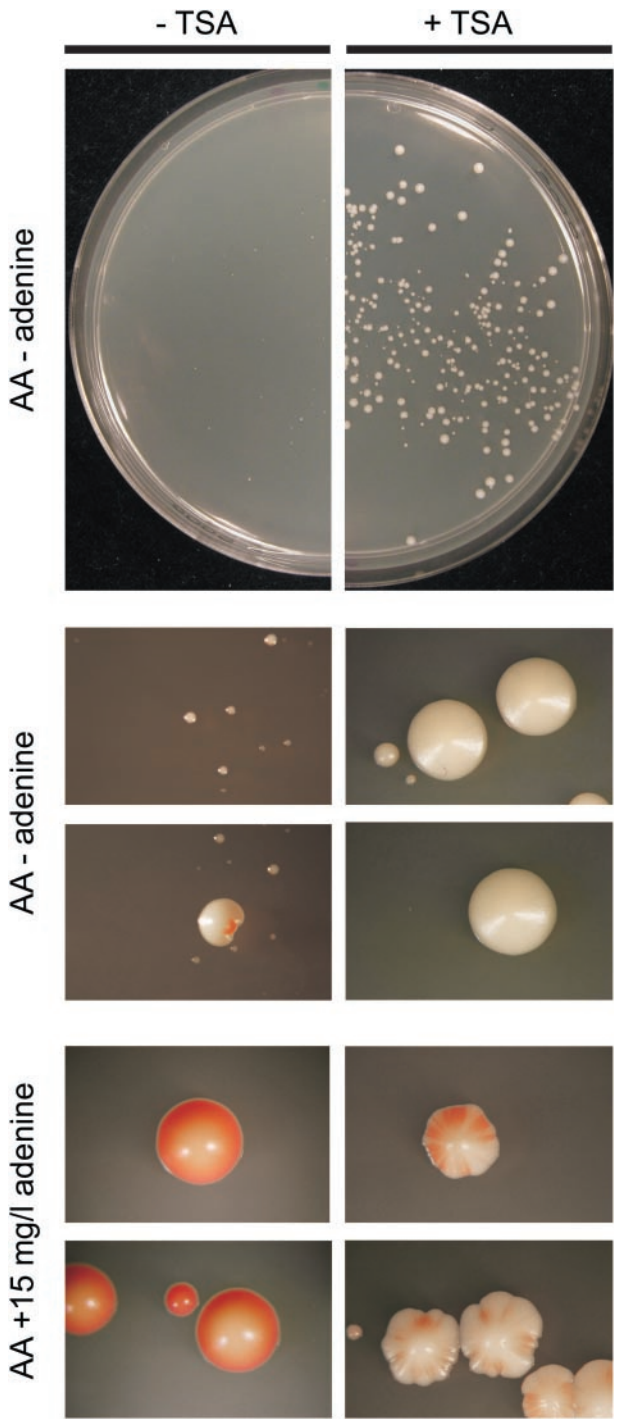

Figure 7. Sensitivity of an ectopic *tlh2-ade6*$^+$ reporter to histone acetylation. PG3263 cells were treated with TSA (+TSA) or mock treated (−TSA), plated on the indicated selective or indicator media, incubated for 4 days at 33°C, and plates were scored and photographed.

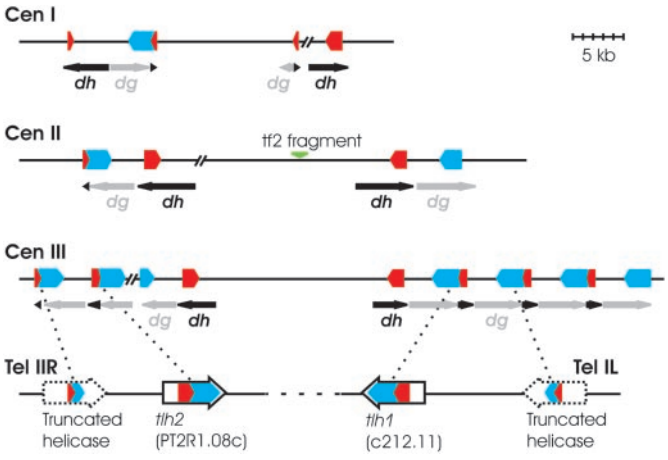

Figure 8. Model for the generation of a centromere by telomere fusion. Partial *tlh* ORFs are found in subtelomeric regions in addition to the full-length genes, suggesting that *tlh* genes were once present in several copies at these sites (dotted arrows). A dashed line shows how a telomeric end to end fusion of the PT2R1 (Tel IIR) and c212 (Tel IL) regions would create a symmetrical structure like those at centromeres.

that such end fusions confer some of the properties required for centromere function in *S.pombe*. The ability of *tlh1* or *tlh2* to induce heterochromatin formation in a context different from telomeres is also demonstrated by their effects at an ectopic site. A similar origin can be imagined for the *cenH* element in the mating-type region. In hemiascomycetes with triplicated mating-type loci, the two silent mating-type cassettes are located in subtelomeric regions (70). The *mat2-P* and *mat3-M* loci might also once have been subtelomeric in an ancestor of *S.pombe* and been internalized together with a *tlh* copy creating the mating-type region.

SUPPLEMENTARY DATA

Supplementary Data are available at NAR Online.

ACKNOWLEDGEMENTS

We thank Rob Martienssen for bringing literature reports of helitrons to our attention and Janne Verhein-Hansen for technical help with some of the experiments. Our research was supported by the Danish Research Council and by a PhD fellowship from the University of Copenhagen to K.R.H. Funding to pay the Open Access publication charges for this article was provided by the Danish Research Council.

Conflict of interest statement. None declared.

REFERENCES

1. Henikoff,S. and Dalal,Y. (2005) Centromeric chromatin: what makes it unique? *Curr. Opin. Genet. Dev.*, **15**, 177–184.
2. Allshire,R. (2004) Centromere and kinetochore structure and function. In Egel,R. (ed.), *The Molecular Biology of Schizosaccharomyce pombe*. Springer-Verlag, Berlin, pp. 149–169.
3. Clarke,L., Amstutz,H., Fishel,B. and Carbon,J. (1986) Analysis of centromeric DNA in the fission yeast *Schizosaccharomyces pombe*. *Proc. Natl Acad. Sci. USA*, **83**, 8253–8257.
4. Nakaseko,Y., Kinoshita,N. and Yanagida,M. (1987) A novel sequence common to centromere regions of *Schizosaccharomyces pombe* chromosomes. *Nucleic Acids Res.*, **12**, 4705–4715.
5. Fishel,B., Amstutz,H., Baum,M., Carbon,J. and Clarke,L. (1988) Structural organization and functional analysis of centromeric DNA in the fission yeast *Schizosaccharomyces pombe*. *Mol. Cell. Biol.*, **8**, 754–763.
6. Chikashige,Y., Kinoshita,N., Nakaseko,Y., Matsumoto,T., Murakami,S., Niwa,O. and Yanagida,M. (1989) Composite motifs and repeat symmetry in *S.pombe* centromeres: direct analysis by integration of *Not*I restriction sites. *Cell*, **57**, 739–751.
7. Murakami,S., Matsumoto,T., Niwa,O. and Yanagida,M. (1991) Structure of the fission yeast centromere cen3: direct analysis of the reiterated inverted region. *Chromosoma*, **101**, 214–221.
8. Wood,V., Gwilliam,R., Rajandream,M.A., Lyne,M., Lyne,R., Stewart,A., Sgouros,J., Peat,N., Hayles,J., Baker,S. *et al.* (2002) The genome sequence of *Schizosaccharomyces pombe*. *Nature*, **415**, 871–880.
9. Clarke,L. and Baum,M.P. (1990) Functional analysis of a centromere from fission yeast: a role for centromere-specific repeated DNA sequences. *Mol. Cell. Biol.*, **10**, 1863–7182.
10. Takahashi,K., Murakami,S., Chikashige,Y., Funabiki,H., Niwa,O. and Yanagida,M. (1992) A low copy number central sequence with strict symmetry and unusual chromatin structure in fission yeast centromere. *Mol. Biol. Cell*, **3**, 819–835.
11. Grewal,S.I. and Klar,A.J. (1997) A recombinationally repressed region between *mat2* and *mat3* loci shares homology to centromeric repeats and regulates directionality of mating-type switching in fission yeast. *Genetics*, **146**, 1221–1238.
12. Grewal,S.I. and Klar,A.J. (1996) Chromosomal inheritance of epigenetic states in fission yeast during mitosis and meiosis. *Cell*, **86**, 95–101.
13. Thon,G. and Friis,T. (1997) Epigenetic inheritance of transcriptional silencing and switching competence in fission yeast. *Genetics*, **145**, 685–696.
14. Nakayama,J., Klar,A.J. and Grewal,S.I. (2000) A chromodomain protein, Swi6, performs imprinting functions in fission yeast during mitosis and meiosis. *Cell*, **101**, 307–317.
15. Hall,I.M., Shankaranarayana,G.D., Noma,K., Ayoub,N., Cohen,A. and Grewal,S.I. (2002) Establishment and maintenance of a heterochromatin domain. *Science*, **297**, 2232–2237.
16. Ayoub,N., Goldshmidt,I., Lyakhovetsky,R. and Cohen,A. (2000) A fission yeast repression element cooperates with centromere-like sequences and defines a mat silent domain boundary. *Genetics*, **156**, 983–994.
17. Partridge,J.F., Scott,K.S., Bannister,A.J., Kouzarides,T. and Allshire,R.C. (2002) cis-acting DNA from fission yeast centromeres mediates histone H3 methylation and recruitment of silencing factors and cohesin to an ectopic site. *Curr. Biol.*, **12**, 1652–1660.
18. Reinhart,B.J. and Bartel,D.P. (2002) Small RNAs correspond to centromere heterochromatic repeats. *Science*, **297**, 1831.
19. Volpe,T.A., Kidner,C., Hall,I.M., Teng,G., Grewal,S.I. and Martienssen,R.A. (2002) Regulation of heterochromatic silencing and histone H3 lysine-9 methylation by RNAi. *Science*, **297**, 1833–1837.
20. Martienssen,R.A., Zaratiegui,M. and Goto,D.B. (2005) RNA interference and heterochromatin in the fission yeast *Schizosaccharomyces pombe*. *Trends Genet.*, **21**, 450–456.
21. Verdel,A., Jia,S., Gerber,S., Sugiyama,T., Gygi,S., Grewal,S.I. and Moazed,D. (2004) RNAi-mediated targeting of heterochromatin by the RITS complex. *Science*, **303**, 672–676.
22. Motamedi,M.R., Verdel,A., Colmenares,S.U., Gerber,S.A., Gygi,S.P. and Moazed,D. (2004) Two RNAi complexes, RITS and RDRC, physically interact and localize to noncoding centromeric RNAs. *Cell*, **119**, 789–802.
23. Cam,H.P., Sugiyama,T., Chen,E.S., Chen,X., FitzGerald,P.C. and Grewal,S.I. (2005) Comprehensive analysis of heterochromatin- and RNAi-mediated epigenetic control of the fission yeast genome. *Nature Genet.*, **37**, 809–819.
24. Partridge,J.F., Borgstrøm,B. and Allshire,R.C. (2000) Distinct protein interaction domains and protein spreading in a complex centromere. *Genes Dev.*, **14**, 783–791.
25. Thon,G. and Verhein-Hansen,J. (2000) Four chromo-domain proteins of *Schizosaccharomyces pombe* differentially repress transcription at various chromosomal locations. *Genetics*, **155**, 551–568.
26. Provost,P., Silverstein,R.A., Dishart,D., Walfridsson,J., Djupedal,I., Kniola,B., Wright,A., Samuelsson,B., Radmark,O. and Ekwall,K. (2002)

Dicer is required for chromosome segregation and gene silencing in fission yeast cells. *Proc. Natl Acad. Sci. USA*, **99**, 16648–16653.
27. Noma,K., Sugiyama,T., Cam,H., Verdel,A., Zofall,M., Jia,S., Moazed,D. and Grewal,S.I. (2004) RITS acts in cis to promote RNA interference-mediated transcriptional and post-transcriptional silencing. *Nature Genet.*, **36**, 1174–1180.
28. Sadaie,M., Iida,T., Urano,T. and Nakayama,J. (2004) A chromodomain protein, Chp1, is required for the establishment of heterochromatin in fission yeast. *EMBO J.*, **23**, 3825–3835.
29. Petrie,V.J., Wuitschick,J.D., Givens,C.D., Kosinski,A.M. and Partridge,J.F. (2005) RNA interference (RNAi)-dependent and RNAi-independent association of the Chp1 chromodomain protein with distinct heterochromatic loci in fission yeast. *Mol. Cell. Biol.*, **25**, 2331–2346.
30. Sugiyama,T., Cam,H., Verdel,A., Moazed,D. and Grewal,S.I. (2005) RNA-dependent RNA polymerase is an essential component of a self-enforcing loop coupling heterochromatin assembly to siRNA production. *Proc. Natl Acad. Sci. USA*, **102**, 152–157.
31. Jia,S., Noma,K. and Grewal,S.I. (2004) RNAi-independent heterochromatin nucleation by the stress-activated ATF/CREB family proteins. *Science*, **304**, 1971–1976.
32. Kim,H.S., Choi,E.S., Shin,J.A., Jang,Y.K. and Park,S.D. (2004) Regulation of Swi6/HP1-dependent heterochromatin assembly by cooperation of components of the mitogen-activated protein kinase pathway and a histone deacetylase Clr6. *J. Biol. Chem.*, **279**, 42850–42859.
33. Cooper,J.P., Nimmo,E.R., Allshire,R.C. and Cech,T.R. (1997) Regulation of telomere length and function by a Myb-domain protein in fission yeast. *Nature*, **385**, 744–747.
34. Mandell,J.G., Bähler,J., Volpe,T.A., Martienssen,R.A. and Cech,T.R. (2005) Global expression changes resulting from loss of telomeric DNA in fission yeast. *Genome Biol.*, **6**, R1.
35. Mandell,J.G., Goodrich,K.J., Bähler,J. and Cech,T.R. (2005) Expression of a RecQ helicase homolog affects progression through crisis in fission yeast lacking telomerase. *J. Biol. Chem.*, **280**, 5249–5257.
36. Bach,M.L. (1987) Cloning and expression of the OMP decarboxylase gene URA4 from *Schizosaccharomyces pombe*. *Curr. Genet.*, **12**, 527–534.
37. Szankasi,P., Heyer,W.D., Schuchert,P. and Kohli,J. (1988) DNA sequence analysis of the ade6 gene of *Schizosaccharomyces pombe*. Wild-type and mutant alleles including the recombination host spot allele ade6-M26. *J. Mol. Biol.*, **204**, 917–925.
38. Lyne,R., Burns,G., Mata,J., Penkett,C.J., Rustici,G., Chen,D., Langford,C., Vetrie,D. and Bähler,J. (2003) Whole-genome microarrays of fission yeast: characteristics, accuracy, reproducibility, and processing of array data. *BMC Genomics*, **4**, 27.
39. Simon,P. (2003) Q-Gene: processing quantitative real-time RT–PCR data. *Bioinformatics*, **19**, 1439–1440.
40. Altschul,S.F., Gish,W., Miller,W., Myers,E.W. and Lipman,D.J. (1990) Basic local alignment search tool. *J. Mol. Biol.*, **215**, 403–410.
41. Thompson,J.D., Higgins,D.G. and Gibson,T.J. (1994) CLUSTAL W: improving the sensitivity of progressive multiple sequence alignment through sequence weighting, position-specific gap penalties and weight matrix choice. *Nucleic Acids Res.*, **22**, 4673–4680.
42. Perrière,G. and Gouy,M. (1996) WWW-query: an on-line retrieval system for biological sequence banks. *Biochimie*, **78**, 364–369.
43. Harper,L., Golubovskaya,I. and Cande,W.Z. (2004) A bouquet of chromosomes. *J. Cell Sci.*, **117**, 4025–4032.
44. Sanchez-Alonso,P. and Guzman,P. (1998) Organization of chromosome ends in *Ustilago maydis*. RecQ-like helicase motifs at telomeric regions. *Genetics*, **148**, 1043–1054.
45. Inglis,P.W., Rigden,D.J., Mello,L.V., Louis,E.J. and Valadares-Inglis,M.C. (2005) Monomorphic subtelomeric DNA in the filamentous fungus *Metarhizium anisopliae* contains a RecQ helicase-like gene. *Mol. Genet. Genomics*, **4**, 79–90.
46. Gao,W., Khang,C.H., Park,S.Y., Lee,Y.H. and Kang,S. (2002) Evolution and organization of a highly dynamic, subtelomeric helicase gene family in the rice blast fungus *Magnaporthe grisea*. *Genetics*, **162**, 103–112.
47. Louis,E.J. and Haber,J.E. (1992) The structure and evolution of subtelomeric Y′ repeats in *Saccharomyces cerevisiae*. *Genetics*, **131**, 559–574.
48. Yamada,M., Hayatsu,N., Matsuura,A. and Ishikawa,F. (1998) Y′-Help1, a DNA helicase encoded by the yeast subtelomeric Y′ element, is induced in survivors defective for telomerase. *J. Biol. Chem.*, **273**, 33360–33366.
49. Lundblad,V. and Blackburn,E.H. (1993) An alternative pathway for yeast telomere maintenance rescues est1-senescence. *Cell*, **73**, 347–360.
50. Teng,S.C. and Zakian,V.A. (1999) Telomere–telomere recombination is an efficient bypass pathway for telomere maintenance in *Saccharomyces cerevisiae*. *Mol. Cell. Biol.*, **19**, 8083–8093.
51. Maxwell,P.H., Coombes,C., Kenny,A.E., Lawler,J.F., Boeke,J.D. and Curcio,M.J. (2004) Ty1 mobilizes subtelomeric Y′ elements in telomerase-negative *Saccharomyces cerevisiae* survivors. *Mol. Cell. Biol.*, **24**, 9887–9898.
52. Mata,J., Lyne,R., Burns,G. and Bähler,J. (2002) The transcriptional program of meiosis and sporulation in fission yeast. *Nature Genet.*, **32**, 143–147.
53. Hansen,K.R., Burns,G., Mata,J., Volpe,T.A., Martienssen,R.A., Bähler,J. and Thon,G. (2005) Global effects on gene expression in fission yeast by silencing and RNA interference machineries. *Mol. Cell. Biol.*, **25**, 590–601.
54. Horn,P.J., Bastie,J.N. and Peterson,C.L. (2005) A Rik1-associated, cullin-dependent E3 ubiquitin ligase is essential for heterochromatin formation. *Genes Dev.*, **19**, 1705–1714.
55. Jia,S., Kobayashi,R. and Grewal,S.I. (2005) Ubiquitin ligase component Cul4 associates with Clr4 histone methyltransferase to assemble heterochromatin. *Nature Cell Biol.*, **7**, 1007–1013.
56. Li,F., Goto,D.B., Zaratiegui,M., Tang,X., Martienssen,R. and Cande,W.Z. (2005) Two novel proteins, Dos1 and Dos2, interact with Rik1 to regulate heterochromatic RNA interference and histone modification. *Curr. Biol.*, **15**, 1448–1457.
57. Thon,G., Hansen,K.R., Altes,S.P., Sidhu,D., Singh,G., Verhein-Hansen,J., Bonaduce,M.J. and Klar,A.J.S. (2005) The Clr7 and Clr8 directionality factors and the Pcu4 cullin mediate heterochromatin formation in the fission yeast *Schizosaccharomyces pombe*. *Genetics,* **171**, 1583–1595.
58. Nimmo,E.R., Pidoux,A.L., Perry,P.E. and Allshire,R.C. (1998) Defective meiosis in telomere-silencing mutants of *Schizosaccharomyces pombe*. *Nature*, **392**, 825–828.
59. Ueno,M., Murase,T., Kibe,T., Ohashi,N., Tomita,K., Murakami,Y., Uritani,M., Ushimaru,T. and Harata,M. (2004) Fission yeast Arp6 is required for telomere silencing, but functions independently of Swi6. *Nucleic Acids Res.*, **32**, 736–741.
60. Thon,G., Bjerling,K.P. and Nielsen,I.S. (1999) Localization and properties of a silencing element near the *mat3-M* mating-type cassette of *Schizosaccharomyces pombe*. *Genetics*, **151**, 945–963.
61. Kapitonov,V.V. and Jurka,J. (2001) Rolling-circle transposons in eukaryotes. *Proc. Natl Acad. Sci. USA*, **98**, 8714–8719.
62. Patterson,T.E., Albrecht,E.B., Nurse,P., Sazer,S. and Stark,G.R. (1999) Effects of genome position and the DNA damage checkpoint on the structure and frequency of sod2 gene amplification in fission yeast. *Mol. Biol. Cell.*, **10**, 2199–2208.
63. Albrecht,E.B., Hunyady,A.B., Stark,G.R. and Patterson,T.E. (2000) Mechanisms of sod2 gene amplification in *Schizosaccharomyces pombe*. *Mol. Biol. Cell*, **11**, 873–886.
64. Mewborn,S.K., Lese Martin,C. and Ledbetter,D.H. (2005) The dynamic nature and evolutionary history of subtelomeric and pericentromeric regions. *Cytogenet. Genome Res.*, **108**, 22–25.
65. Nanda,I., Schrama,D., Feichtinger,W., Haaf,T., Schartl,M. and Schmid,M. (2002) Distribution of telomeric (TTAGGG)(*n*) sequences in avian chromosomes. *Chromosoma*, **111**, 215–227.
66. Uchida,W., Matsunaga,S., Sugiyama,R. and Kawano,S. (2002) Interstitial telomere-like repeats in the *Arabidopsis thaliana* genome. *Genes Genet. Syst.*, **77**, 63–67.
67. Dobigny,G., Ozouf-Costaz,C., Bonillo,C. and Volobouev,V. (2003) Evolution of rRNA gene clusters and telomeric repeats during explosive genome repatterning in *TATERILLUS X* (*Rodentia, Gerbillinae*). *Cytogenet. Genome Res.*, **103**, 94–103.
68. Nakamura,T.M., Cooper,J.P. and Cech,T.R. (1998) Two modes of survival of fission yeast without telomerase. *Science*, **282**, 493–496.
69. Sadaie,M., Naito,T. and Ishikawa,F. (2003) Stable inheritance of telomere chromatin structure and function in the absence of telomeric repeats. *Genes Dev.*, **17**, 2271–2282.
70. Fabre,E., Muller,H., Therizols,P., Lafontaine,I., Dujon,B. and Fairhead,C. (2005) Comparative genomics in hemiascomycete yeasts: evolution of sex, silencing, and subtelomeres. *Mol. Biol. Evol.*, **22**, 856–873.